CHEMISTRY
A EUROPEAN JOURNAL

DOI: 10.1002/chem.200903372

The Torsional Barriers of 2-Hydroxy- and 2-Fluorobiphenyl: Small but Measurable

Andrea Mazzanti,*[a] Lodovico Lunazzi,[a] Renzo Ruzziconi,*[b] Sara Spizzichino,[b] and Manfred Schlosser*[c]

Abstract: By making use of a novel diastereotopicity probe, namely $C(CF_3)_2OH$, it has been possible to measure by very low temperature ^{19}F NMR spectroscopy the elusive aryl–aryl rotation barriers of biphenyls bearing an OH or F group in one *ortho* position. The experimental values (5.4 and 4.4 kcal mol^{-1}, respectively) are matched by those from ab initio calculations (5.3 and 4.3 kcal mol^{-1}, respectively).

Keywords: ab initio calculations · biphenyls · diastereotopicity probes · NMR spectroscopy · steric hindrance

Introduction

The most popular scale for quantifying steric bulk is based on the so-called *A* values,[1–5] which mirror the relative free energies of axially versus equatorially substituted cyclohexanes. Despite its conceptional and experimental appeal, this model is not free from bias. In particular, axially oriented monovalent substituents barely touch the axial hydrogen neighbours at the 3- and 5-positions and thus give rise to only insignificant repulsive forces. As a consequence, the *A* values (hydrogen as reference with $A=0.00$) of fluorine ($A=0.15$), chlorine ($A=0.43$), bromine ($A=0.38$) and iodine ($A=0.43$) are very small compared to methyl ($A=1.70$) or isopropyl ($A=2.15$).

To avoid such a dilemma, the two interacting bonds should encounter each other in a lateral tackling array rather than through parallel contact. The biphenyl core satisfies such geometrical requirements optimally, as the collision angle of 60° mimics realistically the interference of a sterically congestive substituent with the trajectory of a reagent approaching the reaction center (e.g., a nucleophile in an S_N2 reaction). Pioneering work in this respect was accomplished by Sternhell et al.,[6] who assessed the torsional barriers of a large series of 2-substituted biphenyls by variable-temperature ("dynamic" D) NMR spectroscopy monitoring the coalescence of a pair of geminal methyl groups at the 3′-position, incorporated into a dihydroindane ring. Unfortunately, they were unable to decrease the sample temperature below −65 °C. In order to operate in the −65 °C/+185 °C range (corresponding to barriers of 14–22 kcal mol^{-1}) they were obliged to introduce an extra methyl group at the 6′-position of all test compounds. To list steric parameters I^{X-H} of individual substituents X they had to assume additivity of the 2-X/2′-H and 6-H/6′-CH_3 repulsions. In other words, they always had to subtract the same constant I^{CH_3-H} increment from the experimentally found barrier. The underlying additivity postulate is incorrect, however.

Results and Discussion

By adjusting the temperature to as low as −173 °C (100 K) we were able to determine the torsional barriers ("*B* values") of a representative series of biphenyls having a single substituent at an *ortho* position, by employing 3′-isopropyldimethylsilyl as diastereotopicity probe.[7] The examples listed (Table 1) span an unprecedented wide range from moderate size (methyl: *B* 7.4; chloro: *B* 7.7) to fairly bulky groups (*tert*-butyl: *B* 15.5; trimethylammonio: *B* 18.1).[7]

[a] Dr. A. Mazzanti, Prof. L. Lunazzi
Department of Organic Chemistry "A. Mangini"
University of Bologna
Viale Risorgimento 4, 40136 Bologna (Italy)
Fax: (+39) 051-2093654
E-mail: mazzand@ms.fci.unibo.it

[b] Prof. R. Ruzziconi, S. Spizzichino
Chemistry Department, University of Perugia
Via Elce di Sotto 10, 06100 Perugia (Italy)
E-mail: ruzzchor@unipg.it

[c] Prof. M. Schlosser
Institute of Chemical Science and Engineering
Ecole Polytechnique Fédérale (EPFL-BCh)
1015 Lausanne (Switzerland)
E-mail: manfred.schlosser@epfl.ch

Supporting information for this article is available on the WWW under http://dx.doi.org/10.1002/chem.200903372.

Table 1. *B* values of common substituents, as determined by the torsional barriers of biphenyl model compounds,[a] with corresponding *A* values for comparison.[2–4]

Substituent X	*A* values exptl	*B* values exptl[b]	*B* values calcd[c]
H	0.0	–	2.2[d]
CH_3	1.70	7.4[e] (10.8)	7.1
C_2H_5	1.75	8.7[e]	–
$CH(CH_3)_2$	2.15	11.1[e] (13.7)	11.1
$C(CH_3)_3$	4.90	15.5	15.6
$^+N(CH_3)_3$	–	18.1	18.2
$N(CH_3)_2$	2.10	6.9[f] (8.9)	6.8[f]
NH_2	1.20	8.1[f] (10.7)	8.4[f]
NO_2	1.10	7.6 (8.8)	7.8
OCH_3	0.60	5.6 (7.5)	4.5
OCH_2OCH_3	–	5.7	6.1
OH	0.52	–[g] (7.6)	5.3[h]
F	0.15	–[g] (5.7)	4.3[h]
Cl	0.43	7.7[e] (10.2)	7.3
Br	0.38	8.7 (11.3)	8.5
I	0.43	10.0 (12.0)	9.9[i]

[a] *B* values [kcal mol^{-1}] are the torsional barriers of 2-X-biphenyls carrying at the 3′-position generally an isopropyldimethylsilyl group as the diastereotopicity probe. [b] The values in parentheses are taken from ref. [6]. [c] With B3LYP/6-311+G(2d,p)//B3LYP/6-311+G(2d,p).[7] [d] Ref. [8]. [e] Isopropyl was the diastereotopicity probe;[9] see also ref. [10]. [f] The reason why 2-dimethylamino seems to be smaller than 2-amino has to do with the various degrees of n–π conjugative stabilization in the ground and transition states.[7] [g] No decoalescence of the isopropyldimethylsilyl group down to −173 °C. [h] With CCSD(T)/6-31G(d)//CISD(full)/6-31G(d) neglecting the diastereotopicity label at the 3′-position. [i] With B3LYP/DGDZVP//B3LYP/DGDZVP.

However, the challenge presented by the two smallest substituents, hydroxy and fluoro, proved insurmountable. Their torsional barriers can not exceed 5 kcal mol^{-1}, as not even the beginning of decoalescence was observed at −173 °C.[7]

The only hope to solve the problem was to replace the so-far top-performing isopropyldimethylsilyl probe by an even better diastereotopicity sensor, in other words by one showing wider signal splitting of the diastereotopic nuclei. We chose the α-hydroxyhexafluoroisopropyl (HOF_6iPr) group, which we planned to attach to the biphenyl core by nucleophilic addition of a suitable aryl lithium to anhydrous hexafluoroacetone. The sparse literature reports available were contradictory, and thus cast doubt on the practicability of the envisaged approach. Phenylethynylsodium was found to combine cleanly with hexafluoroacetone (in 76% yield),[11] whereas sodium acetylide provided only 16% of impure product.[12] 1,1-Dichloroallyllithium reacted with hexafluoroacetone readily and regioselectively,[13] but 2-(dimethylamino)phenyllithium gave the expected *ortho*-substituted adduct contaminated with considerable amounts of the corresponding *meta* isomer.[14] Despite such inconsistencies, 3-bromophenyllithium, generated from 1,3-dibromobenzene by halogen/metal permutation with *n*-butyllithium, combined smoothly with hexafluoroacetone to afford, after hydrolysis, 1-bromo-3-(α-hydroxyhexafluoroisopropyl)benzene (**1**). Reaction of aryl bromide **1** with 2-methoxymethoxyphenylboronic acid, 2-fluorophenylboronic acid, 2-bromophenylboronic acid or phenylboronic acid under the conditions of Suzuki–Miyaura cross-coupling[15] in the presence of tetrakis(triphenylphosphine)palladium(0)[16] and subsequent acid cleavage afforded 2-hydroxy-3′-(α-hydroxyhexafluoroisopropyl)biphenyl (**2**), 2-fluoro-3′-(α-hydroxyhexafluoroisopropyl)biphenyl (**3**), 2-bromo-3′-(α-hydroxyhexafluoroisopropyl)biphenyl (**4**) and the *ortho*-unsubstituted parent compound 3-(α-hydroxyhexafluoroisopropyl)biphenyl (**5**) in 58, 73, 50 and 70% yield, respectively (Scheme 1).

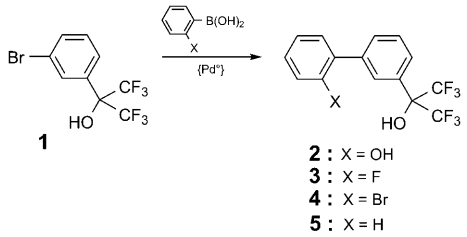

Scheme 1. Preparation of biphenyls **2**–**5** starting from the common precursor **1**.

The new diastereotopicity probe met our expectations. First, the torsional barrier of 2-bromo compound **4** was determined ($B=8.3$). The coincidence with the values previously obtained with 3′-isopropyl[9] and 3′-isopropyldimethylsilyl[7] as probes ($B=8.7$) lies within experimental uncertainty. Next, 2-hydroxy compound **2** and 2-fluoro compound **3** were examined.

The ^1H spectrum of **2** shows that the line representing the phenolic hydroxyl group splits into two signals with 65:35 intensity ratio below −150 °C (Figure 1, left). This is due to restricted rotation around the aryl−$C(CF_3)_2OH$ bond, which makes visible, at this temperature, two different OH signals for two unequally populated conformers. In fact, as observed formerly with similarly bulky 3′-substituents,[17,18] the hydroxyl group of the HOF_6iPr entity will be accommodated in the ring plane either facing the neighbouring aryl (*syn* conformer *sp*-**2**, Scheme 2) or looking away from it (*anti* conformer *ap*-**2**, Scheme 2). The *syn*/*anti* interconversion process requires an activation free energy ($\Delta G^{\neq}$) of 6.1 kcal mol^{-1}, as obtained from the rate constants used for the line-shape simulation (Figure 1, dashed lines).

This process is NMR-invisible in the ^{19}F spectrum of **2**, since the chemical shift difference between the *ap* and *sp* conformers is much smaller than the line widths of the CF_3 signals, which are quite large due to the increased viscosity at such low temperatures. However the effects of two other dynamic processes are detected in the ^{19}F spectrum (Figure 1, right), since the chemical shift separations involved are much larger. These other processes are restricted C−CF_3 rotation (which yields three 1:1:1 lines for the three fluorine atoms) and restricted aryl–aryl rotation (which makes the two CF_3 groups diastereotopic). As a consequence, six lines of equal integrated intensity are expected. These lines, however, are not completely resolved. There-

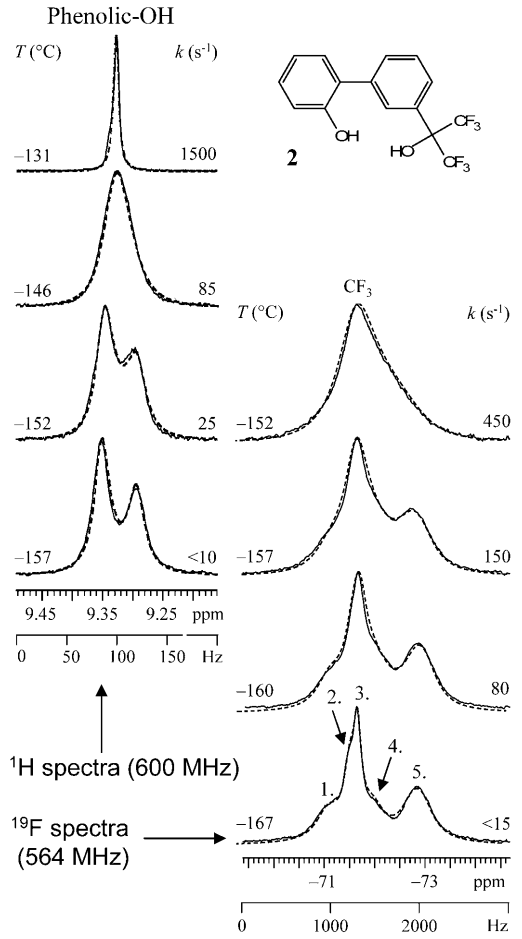

Figure 1. Temperature dependence of the ^{1}H signal of the phenolic OH group (left) and ^{19}F spectrum of the CF_3 groups of **2** in $CBrF_3$ together with the line-shape simulation obtained with the rate constants indicated (dashed lines). The $^{2}J_{FF}$ couplings are smaller than the line width.

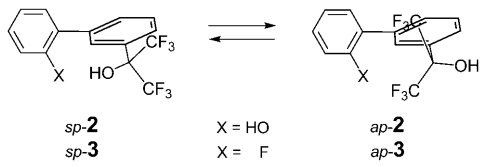

Scheme 2. *syn* and *anti* Conformers of biphenyls **2** and **3**.

fore, only five overlapping lines of different width, and of 1:1:1:1:2 intensity, were detected in the −167 °C spectrum of Figure 1 (right). The experimental intensity distribution, in which the fifth line at $\delta = -72.9$ ppm is twice as intense as the others, was confirmed by the excellent agreement with a line-shape simulation (Figure 1, right, dashed traces).[19]

The rate constants for the aryl–aryl and C−CF_3 rotation appeared to be essentially equal, so that only a single rate constant k results from the simulation. The corresponding barriers for aryl–aryl and C−CF_3 rotations are 5.4 ± 0.3 kcal mol^{-1}. The equality of these two barriers might just be a coincidence, but it is not unreasonable to assume a correlation of the two stereomutations by a common "gear" (or "cogwheel") effect.[20–22]

Analogous behaviour was observed in the ^{19}F spectrum of **3**, in which the signal of the *ortho*-fluorine atom splits below −150 °C into a pair of lines with 60:40 intensity ratio (Figure 2, left) due to the presence of the *sp* and *ap*

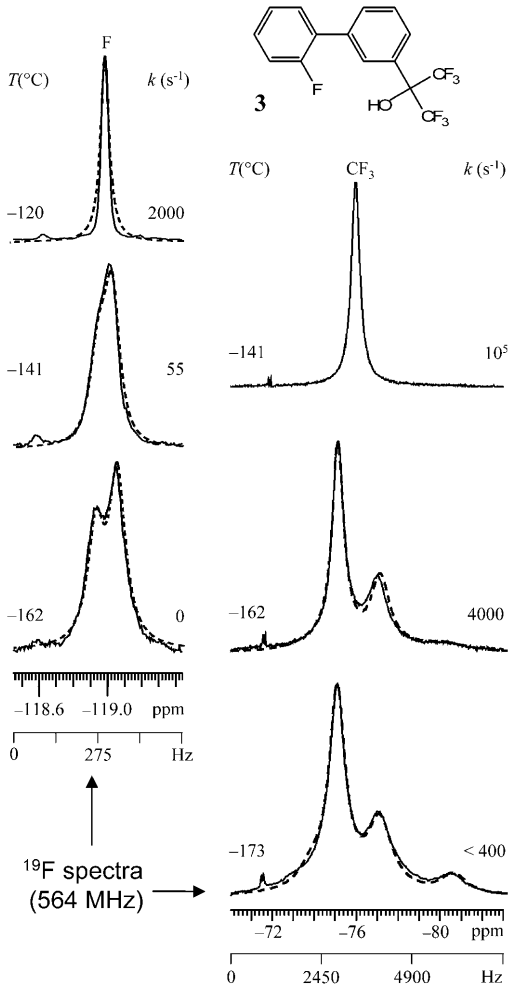

Figure 2. Temperature dependence of the ^{19}F signal of the single phenyl-bound fluorine atom (left) and of the CF_3 groups (right) of **3** in $CBrF_3$ together with the line-shape simulation obtained with the rate constants indicated (dashed lines). The $^{2}J_{FF}$ couplings are smaller than the line width.

conformers (Scheme 2) although the separation of the corresponding signals is as small as 0.1 ppm. The rate constants, obtained by line-shape simulation (dashed lines), lead to a *syn*/*anti* interconversion barrier of $\Delta G^{\ddagger} = 6.4$ kcal mol^{-1}, which is essentially equal, within experimental error (± 0.2 kcal mol^{-1}), to that measured for compound **2**.

The splitting due to *sp* and *ap* conformers is invisible in the CF_3 spectral region, where the signals have line widths larger than the chemical shift separation. At sufficiently low temperatures restricted aryl–aryl and restricted C−CF_3 bond rotation should lead to six equally intense lines, as discussed

for **2**. These six lines partially overlap, whereby three of them yield the line at $\delta = -75.2$ ppm, and two others that at $\delta = -77.2$ ppm. A third isolated single line appears at $\delta = -80.6$ ppm. Consequently three lines having a 3:2:1 integrated intensity ratio are observed at −173 °C (Figure 2, right). The intensity and the varying line widths are perfectly matched by the simulation (dashed trace). Simulations at higher temperatures also correctly reproduce the experimental traces and again suggest that, presumably owing to the above mentioned "gear effect",[20–22] aryl–aryl and C−CF_3 rotation have the same rate constant and the same barrier ($\Delta G^{\neq} = 4.4 \pm 0.3$ kcal mol^{-1}).

To confirm the interpretation of the low-temperature spectra of **2** and **3** we investigated compound **5**, which lacks an *ortho* substituent, so that the aryl–aryl rotation is fast on the NMR timescale at any temperature because the barrier is exceedingly small[8] (2.2 kcal mol^{-1}, Table 1). The dynamic symmetry due to this fast rotation makes compound **5** achiral, and the two CF_3 groups will be enantiotopic and thus equivalent in the NMR spectrum. As a consequence, when C−CF_3 rotation is frozen the ^{19}F single signal would split only into three (rather than six) lines due to the non-equivalence of the three fluorine atoms within each CF_3 group.[23] Indeed, the ^{19}F spectrum of compound **5** at −160 °C displays two lines ($\delta = -76.0$ and −78.4 ppm) with a 4:2 intensity ratio, as expected if two of the three predicted lines overlap at $\delta = -76.6$ ppm (Figure 3). The line-shape simulations, obtained by taking into account three lines with 1:1:1 intensity ratio, provides the C−CF_3 rotation barrier ($\Delta G^{\neq} = 5.4 \pm 0.3$ kcal mol^{-1}). This value is equal to that measured for **2** and quite similar to that of **3**.[24]

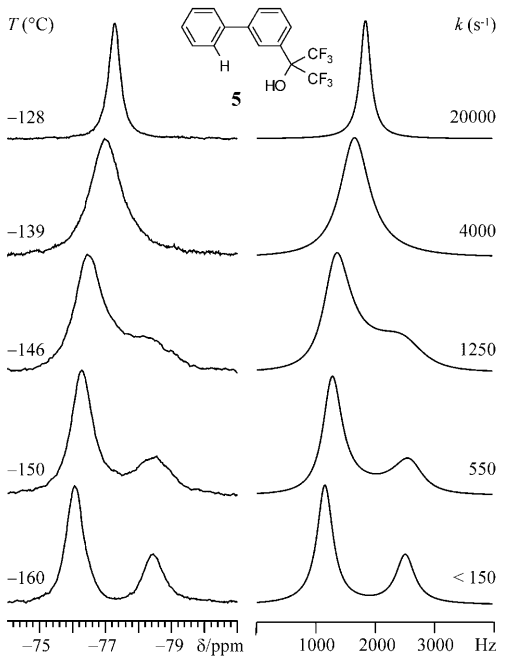

Figure 3. Left: temperature dependence of the ^{19}F signal of the CF_3 groups of **5** in $CBrF_3$ at 564 MHz. Right: line-shape simulation obtained with the rate constants indicated. The $^2J_{FF}$ couplings are smaller than the line width (ca. 350 Hz).[23]

In view of the complexity of our low-temperature spectra we verified the experimental findings by quantum chemical calculations. The torsional barriers of biaryls essentially represent the energy difference between the twisted ground state and the coplanar transition state (where both the steric repulsion of colliding atoms or groups in the *ortho* positions and the stabilizing π conjugation of the parallel-aligned p orbitals attain their maximum)[25] Even when a large basis set is used, the B3LYP functional tends to underestimate the steric barrier with respect to the experimental values,[8] especially in the case of small substituents. For this reason, we optimised the geometries of the ground states and transition states of model compounds **2** and **3** (i.e., 2-hydroxybiphenyl and 2-fluorobiphenyl) at the higher ab initio CISD(full)/6-31G(d) level. Single-point energies were eventually obtained at the even higher CCSD(T)/6-31G(d) level. This gave calculated energy barriers of 5.3 and 4.3 kcal mol^{-1}, in excellent agreement with the experimental values (5.4 and 4.4 kcal mol^{-1}, respectively). This is a strong support for the fact that we actually measured the aryl–aryl rotation barrier.

The smallest barriers ever assessed by dynamic NMR are those of the ring inversions of cyclohexanone,[26] 1,5-cyclooctadiene[26] and *cis*-cyclononene[28] (4.1–4.2 kcal mol^{-1}) and those of the rotations around the single bonds of 2,3-dimethylbutane,[29] chloromethyl methyl ether[30] and 2,2′,6,6′-tetramethyldiphenyl sulfide[21] (4.2–4.3 kcal mol^{-1}). Work in the biphenyl series is hampered by several adverse effects including solubility problems. The smallest torsional barrier so far experimentally assessed in this class of compounds is 5.6 kcal mol^{-1}.[7] The HOF_6*i*Pr group now made it possible to venture to still lower barriers and to establish a new record at 4.4 kcal mol^{-1}. The potential of the new diastereotopicity probe may not yet be exhausted with this success.

Although unintentionally, the present data may stir up once again the old dispute about whether fluorine, as far as its bulkiness is concerned, should be compared to hydrogen or rather to hydroxy.[31,32] If 1.1 kcal mol^{-1} for the interaction of the 6-H/6′-H pair is subtracted from the experimental barriers of 2-hydroxybiphenyl (**2**: 5.4 kcal mol^{-1}) and 2-fluorobiphenyl (**3**: 4.4 kcal mol^{-1}), the remaining 4.3 and 3.3 kcal mol^{-1} account for the 2-OH/2′-H and 2-F/2′-H repulsions, respectively. In other words, fluorine lies between hydrogen and oxygen, but closer to the latter element. On the basis of mere size, fluorine and hydrogen are nevertheless indistinguishable for biological detectors such as enzymes or receptors. In principle one may use the same argument to claim bioisosterism also for hydrogen and hydroxy. However, the recognition pattern of proteins with respect to hydroxylated compounds is generally dominated by the pronounced hydrogen-bond donor and acceptor capacities of the hydroxyl group rather than just by its van der Waals radius.

Experimental Section

Unless stated otherwise, ^{1}H, ^{13}C and ^{19}F NMR spectra were recorded of samples dissolved in $CDCl_3$ at 400, 100 and 376 MHz, respectively. Chemical shifts are given relative to the internal standards tetramethylsilane and trichlorofluoromethane. The purity of all products used in dynamic NMR experiments was tested by gas chromatography on two capillary columns of different polarity [30 m × 0.35 mm × 0.25 μm DB 5MS (5% phenylmethylpolysiloxane) and 30 m × 0.35 mm × 0.25 μm DB23 (50% cyanopropylmethylpolysiloxane)]. A Waters 600 apparatus (with 2487 UV detector) was available for semi-preparative HPLC purification. Elemental analyses of compounds containing more than 10% of fluorine in weight tend to be afflicted with standard deviations exceeding the ordinary error limits of ±0.3%.

Reagents and solvents: Trimethyl borate, 1,3-dibromobenzene, 2-bromophenol, 2-fluorophenylboronic acid, 2-bromophenylboronic acid, chloromethyl methyl ether, tetrakis(triphenylphosphine)palladium and other commercial products were used as received. Tetrahydrofuran and diethyl ether were distilled from KOH pellets in the presence of CuCl and redistilled from sodium wire in the presence of the violet-blue benzophenone/sodium ketyl. All reactions were carried out under an atmosphere of 99.999% pure nitrogen or argon. The aryl–aryl coupling protocols employed for the preparation of products **1**–**5** were elaborated in analogy to literature precedents.[33–35]

2-(3-Bromophenyl)hexafluoroisopropanol (1): Gaseous hexafluoroacetone was produced by cautious addition of its trihydrate to 98% aq. H_2SO_4 at 50 °C and was condensed, through Teflon tubing, into a 50 mL Schlenk tube cooled at −75 °C. In a second Schlenk tube, *n*-butyllithium (1.6 M in hexanes, 13 mL, 21 mmol) was added dropwise over 15 min to a solution of 1,3-dibromobenzene (5.0 g, 21 mmol) in THF (40 mL) at −95 °C. After 5 min hexafluoroacetone was transferred from the first tube, now kept at +25 °C, through a Teflon cannula, ending 5 mm above the liquid surface, into the mixture. After 10 min at −95 °C, the cold bath was removed and the temperature raised to 25 °C. Aq. 5% H_2SO_4 (50 mL) was added and the mixture was extracted with diethyl ether (3 × 25 mL). The extracts were dried with Na_2SO_4 and the solvent evaporated. For purification, the raw material was converted into the methoxymethyl ether [^{1}H NMR: δ = 7.77 (br s, 1H), 7.62 (ddd, J = 8.0, 1.9, 1.0 Hz, 1H), 7.57 (br d, J = 8.0 Hz, 1H), 7.34 (t, J = 8.0 Hz, 1H), 4.85 (s, 2H), 3.55 ppm (s, 3H); MS: *m/z* (%): 368 ([M^++1], 2), 366 ([M^+−1], 2), 308 (65), 306 (67), 227 (100), 253 (99), 207 (80), 157 (59), 61 (54), 45 (100)] and the latter subjected to chromatography (silica gel, eluent 9:1 petroleum ether/diethyl ether mixture) followed by acid cleavage (1:4 v/v trifluoroacetic acid/CH_2Cl_2, 1 h at 25 °C). Upon distillation through a 5 cm Vigreux column, 4.82 g (71%) of bromoarene **1** were collected as a colourless liquid. B.p. 119–121 °C/14 mmHg; ^{1}H NMR: δ = 7.91 (s, 1H), 7.6 (m, 2H), 7.33 (t, J = 8.0 Hz, 1H), 4.06 (s, 1H); ^{13}C NMR: δ = 133.4, 131.5, 130.0, 129.9, 125.2, 122.8, 122.4 (q, J = 286 Hz, 2C), 83.3 ppm (sept, J = 28 Hz); ^{19}F NMR: δ = −75.8 ppm (s); MS *m/z* (%) 324 ([M^++1], 97), 322 ([M^+−1], 98), 285 (2), 283 (2), 255 (99), 253 (99), 204 (38) 185 (100), 183 (100), 157 (33), 155 (31), 145 (31), 69 (48); elemental analysis calcd for $C_9H_5BrF_6O$: C 33.46, H 1.56; found: C 32.89, H 1.58.

2-Hydroxy-3′-(hexafluoro-α-hydroxyisopropyl)biphenyl (2): At −75 °C, *n*-butyllithium (3.9 mL, 1.6 M in hexanes, 6.4 mmol) and, 5 min later, freshly distilled trimethyl borate (1.4 mL, 1.2 g, 12 mmol) were added to 1-bromo-2-(methoxymethoxy)benzene (0.67 g, 3.1 mmol) in THF (50 mL). The volatile substances were replaced by toluene (30 mL), bromoarene **1** (0.68 g, 2.1 mmol), ethanol (30 mL), H_2O (20 mL), Na_2CO_3 (1.0 g, 9.4 mmol) and [$Pd(PPh_3)_4$] (0.074 g, 0.064 mmol). The mixture was heated to 110 °C for 4 h. After cooling, the organic layer was separated and the aqueous phase extracted with diethyl ether (3 × 20 mL). The combined organic phases were dried with Na_2SO_4, the solvent was evaporated and the crude biphenyl treated with trifluoroacetic acid/CH_2Cl_2 (1/4, 10 mL). Saturated aq. $NaHCO_3$ (50 mL) was added with vigorous stirring. The organic phase was separated and dried with Na_2SO_4. After evaporation of the solvent the resulting yellow oil was absorbed on silica gel (5 mL), which, when dry, was poured on top of a column filled with more silica gel (75 mL). Upon elution with diethyl ether/petroleum ether (9/1), 0.41 g (58%) of product **2** was collected as a colourless oil. Hickmann distillation gave biphenyl **2** (0.10 g) as an opalescent gel. B.p. 125–127 °C/0.2 mmHg; ^{1}H NMR: δ = 7.86 (s, 1H), 7.73 (d, J = 7.8 Hz, 1H), 7.6 (m, 2H), 7.3 (m, 2H), 7.02 (t, J = 7.4 Hz, 1H), 6.97 (d, J = 8.0 Hz, 1H), 5.07 (s, 1H), 3.69 ppm (s, 1H); ^{13}C NMR: δ = 152.3, 137.8, 130.9, 130.4, 130.2, 129.5, 129.3, 127.4, 127.3, 125.8, 122.6 (q, J = 286 Hz, 2C), 121.1, 116.1, 83.0 ppm (sept, J = 28 Hz); ^{19}F NMR: δ = −75.8 ppm (s); elemental analysis calcd for $C_{15}H_{10}F_6O_2$: C 53.58, H 3.00; found: C 53.27, H 2.51.

2-Fluoro-3′-(hexafluoro-α-hydroxyisopropyl)biphenyl (3): Ethanol (5 mL), benzene (10 mL), bromoarene **1** (0.50 g, 1.5 mmol), 2.0 M aq. K_2CO_3 (1.5 mL) and [$Pd(PPh_3)_4$] (0.040 g, 0.034 mmol) were added consecutively to 2-fluorophenylboronic acid (0.26 g, 1.9 mmol). The mixture was kept at reflux for 3 h. After cooling, water was added and the mixture extracted with diethyl ether (20 mL). The organic layer was dried with Na_2SO_4 and the solvent evaporated. Chromatography of the residue on silica gel (eluent: diethyl ether/petroleum ether 95/5) afforded a colourless oil. Hickmann distillation gave pure biphenyl **3** (0.370 g, 73%). B.p. 121–123 °C/0.2 mmHg; ^{1}H NMR: δ = 7.91 (s, 1H), 7.72 (d, J = 7.9 Hz, 1H), 7.68 (dsept, J = 7.7 and 1.0 Hz, 1H) 7.54 (t, J = 7.9 Hz, 1H), 7.45 (td, J = 7.7 and 1.8 Hz, 1H), 7.35 (symm. m, 1H), 7.23 (td, J = 7.5 and 1.2 Hz, 1H), 7.17 (ddd, J = 10, 8.2 and 1.1 Hz, 1H), 3.51 ppm (s, 1H); ^{13}C NMR: δ = 159.7 (d, J = 247 Hz), 136.3 (2C), 130.8 (d, J = 20 Hz), 129.5 (d, J = 8.3 Hz), 128.7 (2C), 128.1 (d, J = 13 Hz), 127.2, 125.7, 124.5 (d, J = 3.6 Hz), 122.6 (q, J = 286 Hz, 2C), 116.2 (d, J = 22 Hz), 83.1 ppm (sept, J = 28 Hz); ^{19}F NMR: δ = −75.9 (s, 6F), −118.6 ppm (br s, 1F); MS: *m/z* (%): 338 ([M^+], 100), 269 (100), 251 (36), 199 (100), 172 (92), 152 (28), 99 (38), 85 (32), 69 (16); elemental analysis calcd for $C_{15}H_9F_7O$: C 53.27, H 2.68; found: C 53.37, H 1.98.

2-Bromo-3′-(hexafluoro-α-hydroxyisopropyl)biphenyl (4) was obtained in the same way starting from bromoarene **1** (0.50 g, 1.5 mmol) and 2-bromophenylboronic acid (0.62 g, 3.1 mmol). Upon chromatography of the crude product on silica gel (eluent: petroleum ether/diethyl ether 9/1) impure bromobiphenyl **4** (0.48 g) was isolated. According to mass spectroscopy, it was contaminated mainly by 2-(2-bromophenyl)-3′-(hexafluoro-α-hydroxyisopropyl)biphenyl. A sample (0.14 g) was subjected to preparative HPLC (LiChrospher 100 RP18, 250 × 25 mm × 5 μm column, a mixture of CH_3CN/H_2O (3/2) as eluent, 10 mL min^{-1}) followed by Hickmann distillation, to afford pure bromobiphenyl **4** (0.087 g, 50%). B.p. 143–145 °C/0.2 mmHg; ^{1}H NMR: δ = 7.76 (m, 3H), 7.59 (m, 2H), 7.47 (td, J = 7.6 and 1.1 Hz, 1H), 7.39 (dd, J = 7.6 and 1.6 Hz, 1H), 7.32 (td, J = 7.8 and 1.7 Hz, 1H), 5.99 ppm (s, 1H); ^{13}C NMR: δ = 141.6, 141.4, 133.4, 131.6, 131.4, 129.2, 129.1, 128.3, 128.0, 126.3, 125.7, 123.3 (q, J = 290 Hz, 2C), 122.5, 83.2 ppm (sept, J = 29 Hz); ^{19}F NMR: δ = −75.8 ppm (s); MS *m/z* (%) 400 ([M^++1], 79), 398 ([M^+−1], 78), 331 (21), 329 (21), 313 (13), 311 (13), 250 (24), 181 (91), 152 (100), 76 (33); elemental analysis calcd for $C_{15}H_9BrF_6O$: C 45.14, H 2.27; found: C 44.89, H 2.43.

3-(Hexafluoro-α-hydroxyisopropyl)biphenyl (5): Analogously, biphenyl **5** was obtained by allowing bromoarene **1** (0.48 g, 1.5 mmol) to react with phenylboronic acid (0.23 g. 1.9 mmol). Chromatography on silica gel (eluent: diethyl ether/petroleum ether 95/5), followed by Hickmann distillation, gave pure biphenyl **5** (0.336 g, 70%) as a colourless viscous oil. B.p. 117–119 °C/0.2 mmHg; ^{1}H NMR: δ = 7.96 (s, 1H), 7.7 (m, 2H), 7.6 (m, 2H), 7.54 (t, J = 7.6 Hz, 1H), 7.5 (m, 2H), 7.39 (t, J = 7.5 Hz, 1H), 3.49 ppm (s, 1H); ^{13}C NMR: δ = 141.8, 140.3, 129.8, 129.0 (2C), 128.9 (2C), 127.7, 127.2 (2C) 125.3, 125.2, 122.6 (q, J = 286 Hz, 2C), 83.5 ppm (sept, J = 28 Hz); ^{19}F NMR: δ = −75.9 ppm (s); MS: *m/z* (%): 320 ([M^+, 100), 281 (7), 251 (100), 233 (59), 181 (100), 154 (100), 152 (100), 90 (47), 76 (49); elemental analysis calcd for $C_{15}H_{10}F_6O$: C 56.26, H 3.15. found: C 56.12, H 2.35.

Variable-temperature NMR spectroscopy: Variable-temperature NMR spectra were recorded by using a Varian INOVA spectrometer operating at a field of 14.4 T (600 MHz for ^{1}H). Samples for experiments below −100 °C were prepared at a vacuum line. First a small amount of C_6D_6 or [D_6]acetone (ca. 0.05 mL) was introduced by means of a microsyringe for locking purposes. Next the NMR tube was immersed in liquid nitrogen and evacuated in order to condense about 0.65 mL of $CBrF_3$ (Freon 13B1), which was transferred as gas from a commercial lecture bottle. The tubes were subsequently sealed under reduced pressure (0.01 Torr)

with a methane/oxygen torch. Avoiding any rapid temperature change, they were cautiously warmed to +25 °C, where the Freon develops a pressure of about 12 atm. After 24 h at ambient temperature, the samples can be safely introduced into the probe head of the spectrometer, already cooled to −50 °C. Low-temperature ^{1}H spectra were acquired without spinning by using a 5 mm dual direct probe with a 9000 Hz sweep width, 2.0 μs (20° tip angle) pulse width, 3 s acquisition time and 1 s delay time. ^{19}F spectra were acquired with 90000 Hz sweep width, 2.5 μs (30° tip angle) pulse width, 0.75 s acquisition time and 1 s delay time. A shifted sine bell weighting function[36] equal to the acquisition time was applied before the Fourier transform. Usually 32 to 128 scans were acquired.

When operating the NMR apparatus at low temperature, a flow of nitrogen first passed through a pre-cooling unit adjusted to −50 °C. Then the gas entered into an inox steel heat exchanger immersed in liquid nitrogen and connected to the NMR probe head by a vacuum-insulated transfer line. Gas flows of 10–40 $L\,min^{-1}$ were required to descend to the desired temperature. All the cold parts of the equipment were insulated by neoprene foam. Temperature calibrations were performed before the experiments with a digital thermometer and a Cu/Ni thermocouple (models C9001 and KX2384, respectively, Comark Ltd., Hertfordshire, UK) placed in an NMR tube filled with isopentane. The conditions were kept as identical as possible to the subsequent work; in particular, the sample was not spun and the gas flow was the same as that used during the acquisition of the spectra. The uncertainty in temperature measurements can be estimated as ±2 °C.

Line-shape simulations were performed with a PC version of the QCPE DNMR6 program.[37] Starting from a reasonable guess, after a number of attempts, electronic superimposition of the original and simulated spectrum enabled determination of the most reliable rate constant (examples of data used as an input for the spectral simulations are reported in the Supporting Information). The rate constants thus obtained at various temperatures afforded the free energy of activation $\Delta G^{\neq}$ for bond rotation by applying the Eyring equation.[38] In all cases investigated, $\Delta G^{\neq}$ was found to be invariant in the temperature range investigated. This implies a negligible activation entropy $\Delta S^{\neq}$.[39]

Quantum-chemical calculations: A complete conformational search was preliminarily carried out by means of the molecular mechanics force field (MMFF)[40] by using the Monte-Carlo method implemented in the package TITAN 1.0.5.[41] The most stable conformers identified were subsequently energy-minimised by DFT or ab initio calculations. The whole computational work was performed with the Gaussian 03 (rev. E.01) series of programs[42] on a Dell Poweredge 2900 server, equipped with two quad-core Xeon X5355 processors operating at 2.66 GHz. The operating system was Red Hat Enterprise Linux 5.0. The standard geometry optimisation algorithm ("Berny algorithm") included in Gaussian 03 was used.[43] All DFT calculations employed the B3LYP hybrid HF-DFT method[44,45] and the 6-31G(d) or 6-311+G(d,p) basis set. Harmonic vibrational frequencies were calculated for all stationary points. As revealed by the frequency analysis, imaginary frequencies were absent in all ground states, whereas just one imaginary frequency was associated with each transition state. Visual inspection of the corresponding normal modes[46] validated the identification of the transition states. In the cases of the model systems 2-fluorobiphenyl and 2-hydroxybiphenyl, calculations were performed at the ab initio CISD(full)/6-31G(d) level, including frequency analysis. Single-point energies were then obtained, without frequency analysis, at the CCSD(T)/6-31G(d) level.

The energies listed in Table 1 and those of **2** and **3** represent total electronic energies. In general, these give the best fit with experimental DNMR data.[47] Therefore, the computed values have not been corrected for zero-point energy contributions or other thermodynamic parameters. This avoids artefacts that might result from the inevitably ambiguous choice of an adequate reference temperature, from empirical scaling factors to which one has often to resort for better matching of experimental and theoretical data[48] and from the idealization of low-frequency vibrators as harmonic oscillators (particularly important in the present case, where one third of the calculated frequencies fall in the range 500–600 cm^{-1}).[49]

Acknowledgements

This work was supported by the Universities of Perugia and Bologna, the Ministero dell'Istruzione, Università e Ricerca (MIUR, COFIN contracts nr. 2004033322 and 2005035330) and the Schweizerische Nationalfonds zur Förderung der wissenschaftlichen Forschung, Bern (grant 20-100′336-02).

[1] S. Winstein, N. J. Holness, *J. Am. Chem. Soc.* **1955**, *77*, 5562–5578.
[2] J. A. Hirsch, *Top. Stereochem.* **1967**, *1*, 199–222.
[3] F. A. L. Anet, J. Krane, W. Kitching, D. Dodderel, D. Praeger, *Tetrahedron Lett.* **1974**, *15*, 3255–3258.
[4] C. H. Bushweller in *Conformational Behavior of Six-Membered Rings* (Ed.: E. Juaristi), VCH, Weinheim, **1995**, pp. 25–58.
[5] E. Kleinpeter, F. Taddei, P. Wacker, *Chem. Eur. J.* **2003**, *9*, 1360–1368.
[6] G. Bott, L. D. Field, S. Sternhell, *J. Am. Chem. Soc.* **1980**, *102*, 5618–5626.
[7] R. Ruzziconi, S. Spizzichino, L. Lunazzi, A. Mazzanti, M. Schlosser, *Chem. Eur. J.* **2009**, *15*, 2645–2652.
[8] F. Grein, *J. Phys. Chem. A* **2002**, *106*, 3823–3827.
[9] A. Mazzanti, L. Lunazzi, M. Minzoni, J. E. Anderson, *J. Org. Chem.* **2006**, *71*, 5474–5481.
[10] D. Casarini, L. Lunazzi, M. Mancinelli, A. Mazzanti, C. Rosini, *J. Org. Chem.* **2007**, *72*, 7667–7676.
[11] L. L. Knunyants, T.-Y. Chen, N. P. Gambaryan, *Izv. Akad. Nauk SSSR Ser. Khim.* **1960**, 686–692; [*Chem. Abstr.* **1960**, *54*, 117955].
[12] H. E. Simmons, D. W. Wiley, *J. Am. Chem. Soc.* **1960**, *82*, 2288–2296.
[13] D. Seyferth, G. J. Murphy, B. Mauze, *J. Am. Chem. Soc.* **1977**, *99*, 5317–5330.
[14] A. R. Lepley, W. A. Khan, A. B. Giumanini, A. G. Giumanini, *J. Org. Chem.* **1966**, *31*, 2047–2051.
[15] P. Wawrzyniak, J. Heinicke, *Tetrahedron Lett.* **2006**, *47*, 8921–8924.
[16] M. Nishimura, M. Ueda, N. Miyaura, *Tetrahedron* **2002**, *58*, 5779–5787.
[17] D. Casarini, C. Coluccini, L. Lunazzi, A. Mazzanti, *J. Org. Chem.* **2005**, *70*, 5098–5102.
[18] D. Casarini, C. Coluccini, L. Lunazzi, A. Mazzanti, *J. Org. Chem.* **2006**, *71*, 4490–4496.
[19] An acceptable line-shape simulation could not be obtained if separate lines (65:35 intensity ratio) for the *sp* and *ap* conformers were considered. This confirms that in the CF_3 region the corresponding chemical-shift separation is smaller than the line width.
[20] a) K. Mislow, *Acc. Chem. Res.* **1976**, *9*, 26–33; b) C. Roussel, A. Lidén, M. Chanon, J. Metzger, J. Sandström, *J. Am. Chem. Soc.* **1976**, *98*, 2847–2852; c) H. Iwamura, K. Mislow, *Acc. Chem. Res.* **1988**, *21*, 175–182; d) I. Columbus, S. E. Biali, *J. Org. Chem.* **1994**, *59*, 3402–3407.
[21] a) D. Casarini, S. Grilli, L. Lunazzi, A. Mazzanti, *J. Org. Chem.* **2001**, *66*, 2757–2763, and references therein; b) S. Grilli, L. Lunazzi, A. Mazzanti, *J. Org. Chem.* **2001**, *66*, 4444–4446.
[22] D. K. Frantz, K. K. Baldridge, J. K. Siegel, *Chimia* **2009**, *63*, 201–204.
[23] As observed in the case of compounds **2** and **3** the signals of the *sp* and *ap* conformers have shift differences too small to be detected in the CF_3 spectral region.
[24] Although the experimental errors are relatively large, the fact that the C–CF_3 rotation barrier appears to be slightly smaller in **3** with respect to **5** might support the hypothesis of a possible correlated rotation. It is known, in fact, that such a process reduces the values of the two isolated barriers.[20–22]
[25] M. P. Johansson, J. Olsen, *J. Chem. Theory Comput.* **2008**, *4*, 1460–1471.
[26] F. A. L. Anet, G. N. Chmurni, J. Krane, *J. Am. Chem. Soc.* **1973**, *95*, 4423–4424.
[27] F. A. L. Anet, L. Kozerski, *J. Am. Chem. Soc.* **1973**, *95*, 3407–3408.

[28] D. M. Pawar, S. D. Miggins, S. V. Smith, E. A. Noe, *J. Org. Chem.* **1999**, *64*, 2418–2421.
[29] L. Lunazzi, D. Macciantelli, F. Bernardi, K. U. Ingold, *J. Am. Chem. Soc.* **1977**, *99*, 4573–4576.
[30] F. A. L. Anet, I. Yavari, *J. Am. Chem. Soc.* **1977**, *99*, 6752–6753.
[31] B. E. Smart, *Organofluorine Chemistry : Principles and Commercial Applications* (Eds.: R. E. Banks, B. E. Smart, J. C.Tatlow), Plenum Press, New York, **1994**, pp. 57–88.
[32] M. Schlosser in *Enantiocontrolled Synthesis of Fluoro-Organic Compounds: Stereochemical Challenges and Biomedical Targets* (Ed.: V. A. Soloshonok), Wiley, New York, **1999**, pp. 613–659.
[33] K. Tamao, K. Sumitani, M. Kumada, *J. Am. Chem. Soc.* **1972**, *94*, 4374–4376.
[34] N. G. Andersen, S. P. Maddaford, B. A. Keay, *J. Org. Chem.* **1996**, *61*, 9556–9559.
[35] L. Lunazzi, A. Mazzanti, A. M. Álvarez, *J. Org. Chem.* **2000**, *65*, 3200–3206.
[36] T. D. W. Claridge, *High-Resolution NMR Techniques in Organic Chemistry*, Pergamon, Oxford, **1999**, p. 71.
[37] "DNMR6: Calculation of NMR Spectra Subject to the Effects of Chemical Exchange", J. H. Brown, C. H. Bushweller, *QCPE Bull.* **1983**, *3*, 103–103.
[38] H. Eyring, *Chem. Rev.* **1935**, *17*, 65–77.
[39] a) S. Hoogasian, C. H. Bushweller, W. G. Anderson, G. Kingsley, *J. Phys. Chem.* **1976**, *80*, 643–648; b) L. Lunazzi, G. Cerioni, K. U. Ingold, *J. Am. Chem. Soc.* **1976**, *98*, 7484–7488; c) M. A. Cremonini, L. Lunazzi, G. Placucci, R. Okazaki, G. Yamamoto, *J. Am. Chem. Soc.* **1990**, *112*, 2915–2921; d) D. Casarini, C. Rosini, S. Grilli, L. Lunazzi, A. Mazzanti, *J. Org. Chem.* **2003**, *68*, 1815–1820; e) L. Lunazzi, M. Mancinelli, A. Mazzanti, *J. Org. Chem.* **2007**, *72*, 5391–5394.
[40] T. A. Halgren, *J. Comput. Chem.* **1996**, *17*, 490–519.
[41] Package TITAN 1.0.5, Wavefunction Inc., Irvine.
[42] Gaussian 03, Revision E.01, M. J. Frisch, G. W. Trucks, H. B. Schlegel, G. E. Scuseria, M. A. Robb, J. R. Cheeseman, J. A. Montgomery, Jr., T. Vreven, K. N. Kudin, J. C. Burant, J. M. Millam, S. S. Iyengar, J. Tomasi, V. Barone, B. Mennucci, M. Cossi, G. Scalmani, N. Rega, G. A. Petersson, H. Nakatsuji, M. Hada, M. Ehara, K. Toyota, R. Fukuda, J. Hasegawa, M. Ishida, T. Nakajima, Y. Honda, O. Kitao, H. Nakai, M. Klene, X. Li, J. E. Knox, H. P. Hratchian, J. B. Cross, V. Bakken, C. Adamo, J. Jaramillo, R. Gomperts, R. E. Stratmann, O. Yazyev, A. J. Austin, R. Cammi, C. Pomelli, J. W. Ochterski, P. Y. Ayala, K. Morokuma, G. A. Voth, P. Salvador, J. J. Dannenberg, V. G. Zakrzewski, S. Dapprich, A. D. Daniels, M. C. Strain, O. Farkas, D. K. Malick, A. D. Rabuck, K. Raghavachari, J. B. Foresman, J. V. Ortiz, Q. Cui, A. G. Baboul, S. Clifford, J. Cioslowski, B. B. Stefanov, G. Liu, A. Liashenko, P. Piskorz, I. Komaromi, R. L. Martin, D. J. Fox, T. Keith, M. A. Al-Laham, C. Y. Peng, A. Nanayakkara, M. Challacombe, P. M. W. Gill, B. Johnson, W. Chen, M. W. Wong, C. Gonzalez, J. A. Pople, Gaussian Inc., Wallingford, CT, **2004**.
[43] C. Peng, P. Y. Ayala, H. B. Schlegel, M. J. Frisch, *J. Comput. Chem.* **1996**, *17*, 49–56.
[44] A. D. Becke, *J. Chem. Phys.* **1993**, *98*, 5648–5652.
[45] C. Lee, W. Yang, R. G. Parr, *Phys. Rev. B* **1988**, *37*, 785–789.
[46] Gaussview 4.1.2, Gaussian Inc., Wallingford CT, **2006**.
[47] P. Y. Ayala, H. B. Schlegel, *J. Chem. Phys.* **1998**, *108*, 2314–2325.
[48] C. F. Tormena, R. Rittner, R. J. Abraham, E. A. Basso, B. C. Fiorin, *J. Phys. Org. Chem.* **2004**, *17*, 42–48.
[49] M. W. Wong, *Chem. Phys. Lett.* **1996**, *256*, 391–399.

Received: December 9, 2009
Revised: March 25, 2010
Published online: June 22, 2010

